Analysis of a Semi-Blind Beamspace-Time Interference Cancellation for WCDMA Systems in Microcellular Environments

Ivan R.S. Casella[1,3], Elvino S. Sousa[2] and Paul Jean E. Jeszensky[3]

[1] *Centro de Pesquisa e Desenvolvimento de Informática e Automação - CPDIA - icasella@uol.com.br*

[2] *Department of Electrical and Computer Engineering - University of Toronto - es.sousa@utoronto.ca*

[3] *Laboratório de Comunicações e Sinais - Universidade de São Paulo - pjj@lcs.poli.usp.br*

Abstract - In this paper, we investigate the performance of a semi-blind spatial-temporal beamforming receiver for an asynchronous high data rate direct sequence wideband code division multiple access (DS-WCDMA) system in a microcellular environment. The presented receiver uses subspace channel identification to perform joint channel equalization, multipath energy combination and spatial interference cancellation. The simulation results show a significant performance improvement and reduction of required training symbols when compared against a receiver employing a training-based spatial-temporal recursive least squares (RLS) beamformer.

I. Introduction

A major problem arising from high data rate DS-WCDMA systems (where the delay spread of the channel is much greater than the chip duration) is the severe inter-symbol interference (ISI) due to the multipath nature of the wireless channels, in addition to the multiple access interference (MAI), which is inherent to any non-orthogonal CDMA system and causes the near-far effect.

One promising method to combat these problems is to employ antenna arrays [1, 2, 3]. In general, the multipath signals arrive at the receiver with different angles-of-arrival (AOA), allowing an antenna array to exploit this spatial signature and provide increased space diversity to combat deep fades that occur in the wireless channels. By using this extra degree of freedom, MAI that are spatially separated from the signal-of-interest (SOI) can also be suppressed.

However, the use of space-only processing does not allow for elimination of interference received at the same or similar direction to the desired user and to combine multipath energy. One solution to overcome these limitations is the use of spatial-temporal beamforming. If the desired signal and interference have different temporal or spatial signatures, space-time processing can improve significantly the signal-to-noise ratio (SNR).

In [4], a semi-blind spatial-temporal beamforming receiver based on the SBCMACI (semi-blind constant modulus algorithm with channel identification) [5] was initially presented. The algorithm uses the constant modulus property of the transmitted signal and performs semi-blind subspace channel identification as a precursor to semi-blind equalization. The resulting receiver allows for coherent combination of the desired signal multipath, cancellation of the interfering users, removal of phase ambiguities present in blind algorithms and significant reduction of the required number of training symbols.

In 3rd generation cellular systems, hierarchical microcell-macrocell architecture has been proposed to offer a wide range of services in different environments [6]. Macrocells provide continuous umbrella coverage to high mobility users in a wide area while microcells can offer high spectrum efficiency and achieve strategic coverage to low mobility users in areas with high traffic capacity using low elevation antennas with low transmit power [7]. However, due to the frequency reuse factor equal to one, the use of the hierarchical architecture brings some problems as cross-layer interference.

The use of spatial-temporal antenna array receivers in the microcells can also mitigate this problem, offering efficient handover, capacity enhancement, and reduction of near-far effect between layers of the hierarchical cellular architectures [8].

Due to these observations, we investigate in this paper the performance of the semi-blind SBCMACI spatial-temporal beamforming receiver in a microcell with low mobility and high data rate users. In section VII, comparison against a receiver employing the training-based RLS spatial-temporal beamformer is performed to verify the advantages of the presented semi-blind receiver.

The paper is organized as follows: system model is presented in section II; channel model is presented in section III; LS optimization and semi-blind subspace channel identification in section IV; SBCMACI and RLS beamspace-time algorithms in sections V and VI, respectively; simulation results in section VII and conclusion in section VIII.

II. System Model

We consider the reverse link of an asynchronous DS-CDMA system employing complex spreading [9] and QPSK data modulation to reduce peak-average ratio and achieve better bandwidth occupation. There are *M* users in

the system and each user may transmit N_b data symbols per packet over assumed stationary conditions. It is also assumed that the receiver employs an antenna array consisting of A identical elements equally-spaced by $\lambda_{ant}/2$, where λ_{ant} is the carrier frequency wavelength.

Considering that the inverse signal bandwidth is large compared to the travel time across the array, the complex envelopes of the signals received by different antenna elements from a given path are identical except for phase and amplitude differences [3]. The AOA of the lth multipath signal from the mth user is θ_m^l and $\mathbf{a}(\theta_m^l)$ is the array response vector (spatial signature vector) to the multipath signal arriving from the direction θ_m^l, with $\mathbf{a}(\theta_m^l) = [a_1(\theta_m^l), \cdots, a_A(\theta_m^l)]^T$.

We can represent the reverse link baseband complex signal in the following vector form:

$$\mathbf{r}(t) = \sum_{m=1}^{M} \sum_{k=0}^{N_b-1} \sqrt{\gamma_m} \cdot b_m(k) \cdot \mathbf{h}_m(t - kT_s) + \mathbf{v}(t) \quad (1)$$

Where $\mathbf{r}(t) = [r_1(t), \cdots, r_A(t)]^T$; γ_m is the transmitted signal power of the mth user; T_s is the symbol duration; $b_m(k) = (b_{m,k}^I + jb_{m,k}^Q)/\sqrt{2}$ is the information symbol of the mth user at time k with $b_{m,k}^I, b_{m,k}^Q \in \{+1, -1\}$; $\mathbf{v}(t) = [v^1(t), \cdots, v^A(t)]^T$ is a complex white Gaussian noise vector with variance σ^2 and $\mathbf{h}_m(t) = [h_m^1(t), \cdots, h_m^A(t)]^T$ is the normalized complex signature waveform vector of the mth user, described by:

$$\mathbf{h}_m(t) = \sum_{n=0}^{G-1} c_m(n) \cdot \mathbf{p}_m(t - nT_c), \ 0 \le t \le T_s$$

Where T_c is the chip duration; $G = T_s/T_c$ is the processing gain; $c_m(n) = (\upsilon_{m,n}^I + j\upsilon_{m,n}^Q)/\sqrt{2G}$ is the complex signature sequence (or spreading code) of the mth user at time n with $\upsilon_{m,n}^I, \upsilon_{m,n}^Q \in \{+1, -1\}$ and $\mathbf{p}_m(t) = [p_m^1(t), \cdots, p_m^A(t)]^T$ is the chip waveform vector of the mth user that has been filtered at the transmitter and receiver and distorted by the multipath channel. We can model $\mathbf{p}_m(t)$ as:

$$\mathbf{p}_m(t) = \sum_{l=0}^{L_m-1} \beta_m^l \cdot \mathbf{a}(\theta_m^l) \cdot \psi(t - \tau_m^l)$$

Where L_m is the number of multipath components for the mth user; β_m^l and τ_m^l are the complex gain and time delay of the lth path of the mth user; and $\psi_{chip}(t)$ is the filtered chip waveform, which includes the effect of the transmitter and receiver filter. Finally, sampling the received signal at chip rate and assuming $T_c = 1$, we obtain the following discrete-time signal:

$$\mathbf{r}(n) = \sum_{m=1}^{M} \sqrt{\gamma_m} \sum_{k=0}^{N_b-1} b_m(k) \cdot \mathbf{h}_m(n - kG) + \mathbf{v}(n) \quad (2)$$

We consider that the receiver is in perfect synchronization with the strongest multipath component, l_m, of the desired user m ($\tau_m^{l_m} = 0$) and that each of the A stacked impulse responses of $\mathbf{p}_m(n)$ is FIR with order q_m such that $\lceil \tau_m^{\max}/T_c \rceil \le q_m \le (L-1) \cdot G_p$, where $\tau_m^{\max}$ is the maximum delay spread experienced by the mth user and L is some integer. So, we can write the discrete-time received signal corresponding to the kth symbol as:

$$\mathbf{r}_s(k) = [\mathbf{H}(L-1), \cdots, \mathbf{H}(0)] \cdot [\mathbf{b}(k-L+1)^T, \cdots, \mathbf{b}(k)^T]^T + \mathbf{v}_s(k) \quad (3)$$

Where

$$\mathbf{r}_s(k) = [\mathbf{r}(k \cdot G)^T, \cdots, \mathbf{r}((k+1) \cdot G - 1)^T]^T$$

$$\mathbf{H}(l) = \begin{bmatrix} \mathbf{h}_1(l \cdot G) & \cdots & \mathbf{h}_M(l \cdot G) \\ \vdots & & \vdots \\ \mathbf{h}_1((l+1) \cdot G - 1) & \cdots & \mathbf{h}_M((l+1) \cdot G - 1) \end{bmatrix}$$

$$\mathbf{b}(k) = [b_1(k), \cdots, b_M(k)]^T$$

$$\mathbf{v}_s(k) = [\mathbf{v}(k \cdot G)^T, \cdots, \mathbf{v}((k+1) \cdot G - 1)^T]^T$$

In some cases, depending on the channel length, number of users (M), processing Gain (G) and number of antenna elements (A), it might be necessary to process more than one received vector at a time in order to estimate the kth symbol [5]. Stacking μ consecutive symbols ($\mu \ge 2$), we can define the vector that will be processed, $\mathbf{r}_\mu(k)$, as:

$$\mathbf{r}_\mu(k) = \mathbf{H}_\mu \cdot \mathbf{b}_\mu(k) + \mathbf{v}_\mu(k); \quad (4)$$

Where

$$\mathbf{r}_\mu(k) = [\mathbf{r}_s(k)^T, \cdots, \mathbf{r}_s(k+\mu-1)^T]^T$$

$$\mathbf{b}_\mu(k) = [\mathbf{b}(k)^T, \cdots, \mathbf{b}(k+\mu-1)^T]^T$$

$$\mathbf{v}_\mu(k) = [\mathbf{v}_s(k)^T, \cdots, \mathbf{v}_s(k+\mu-1)^T]^T$$

$$\mathbf{H}_\mu = \begin{bmatrix} \mathbf{H}(L-1) & \cdots & \mathbf{H}(0) & \cdots & 0 \\ \vdots & \ddots & \ddots & \ddots & \vdots \\ 0 & \cdots & \mathbf{H}(L-1) & \cdots & \mathbf{H}(0) \end{bmatrix}$$

III. Channel Model

In this paper, we represent the microcellular multipath propagation channel for each user by the geometrically based single bounced elliptical model (GBSBEM) [10]. In the GBSBEM, it is assumed that the scatterers between the base-station and each user are uniformly distributed within an ellipse. This model is suitable to microcell and picocell environments where antenna heights are low and multipath scattering can occur near the base station or near the mobile with same probability [10]. We can obtain β_m^l,

τ_m^l and θ_m^l of section II, using the procedures presented in [10]. The resulting joint probability density function of AOA and TOA (time of arrival) is given by:

$$f_{\tau,\theta}(\tau_m^l,\theta_m^l)=\begin{cases}\dfrac{\left(d_m^2-\tau_m^{l\,2}c_v^2\right)\cdot\left(d_m^2c_v-2\tau_m^l c_v^2 d_m\cos(\theta_m^l)+\tau_m^{l\,2}c_v^3\right)}{4\pi a_m^{\max}b_m^{\max}\left(d_m\cos(\theta_m^l)-\tau_m^l c_v\right)^3}, & d_m^2/c_v<\tau_m^l\le\tau_m^{\max}\\ 0, & otherwise\end{cases} \quad (5)$$

Where c_v is the speed of light, d_m is the distance of the mth user to the base-station, $a_m^{\max}=c_v\tau_m^{\max}/2$ and $b_m=\sqrt{c_m^2\tau_m^{\max\,2}-d_m^2}$ are the major and minor axes of the ellipse containing the scatterers for the mth user.

In Fig.1 and Fig.2, we present the joint AOA-TOA probability density function and the AOA and TOA histograms, respectively, obtained by evaluating 100.000 scatterers for $d_m=500$ and $\tau_m^{\max}=2d_m/c_v$ [10]. The plots show that there is a high concentration of scatterers near the line of sight with relatively small delays.

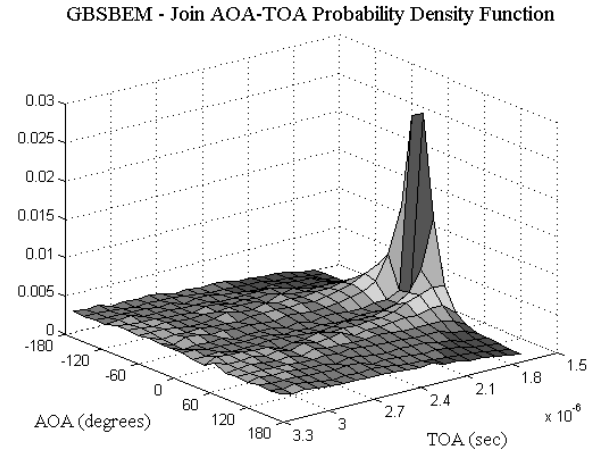

Figure 1 Join AOA-TOA Probability Density Function ($d_m=500$ and $\tau_m^{\max}=2d_m/c_v$)

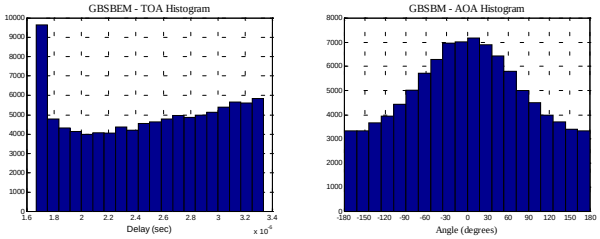

Figure 2 Histograms of AOA and TOA ($d_m=500$ and $\tau_m^{\max}=2d_m/c_v$)

IV. LS Optimization and Semi-Blind Subspace Channel Identification

We can obtain an optimum spatial-temporal weight vector, $\hat{\mathbf{w}}_m$, in the LS sense that provides appropriate beam pattern to the desired user (user m) by [13]:

$$\hat{\mathbf{w}}_m=\underbrace{\left(\frac{1}{N_t}\sum_{k=0}^{N_t-1}\mathbf{r}_\mu(k)\cdot\mathbf{r}_\mu^H(k)\right)^{-1}}_{\hat{\mathbf{R}}_{N_{train}}}\cdot\underbrace{\left(\frac{1}{N_t}\sum_{k=0}^{N_t-1}b_m^*(k)\cdot\mathbf{r}_\mu(k)\right)}_{\hat{\mathbf{p}}_{N_{train}}^m} \quad (6)$$

It is also possible to determine $\hat{\mathbf{P}}_{N_{train}}^m$ by performing channel identification. This procedure allows to work at chip level, increasing the amount of available training data and the estimation accuracy.

As shown in [11], it is possible to perform channel identification based on eigendecomposition of the estimated autocorrelation matrix, $\hat{\mathbf{R}}_{N_b}$, as follows:

$$\hat{\mathbf{R}}_{N_b}=\frac{1}{N_b}\sum_{k=0}^{N_b-1}\mathbf{r}_\mu(k)\cdot\mathbf{r}_\mu^H(k)$$
$$=\begin{bmatrix}\hat{\mathbf{U}}_s & \hat{\mathbf{U}}_n\end{bmatrix}\cdot\begin{bmatrix}\hat{\mathbf{\Lambda}}_s & \\ & \hat{\mathbf{\Lambda}}_n\end{bmatrix}\cdot\begin{bmatrix}\hat{\mathbf{U}}_s & \hat{\mathbf{U}}_n\end{bmatrix}^H \quad (7)$$

Where $\hat{\mathbf{U}}_s=[\hat{\mathbf{u}}_1,\cdots,\hat{\mathbf{u}}_\xi]$, $\hat{\mathbf{U}}_n=[\hat{\mathbf{u}}_{\xi+1},\cdots,\hat{\mathbf{u}}_{ANM}]$, $\hat{\mathbf{\Lambda}}_s$ and $\hat{\mathbf{\Lambda}}_n$ contains the estimated signal space eigenvectors, the estimated noise space eigenvectors and the corresponding eigenvalues for the signal and noise space vectors respectively. ξ is the dimensionality of the signal space (rank of $\mathbf{H}_\mu$) which can be estimated using the MDL criterion [12].

In DS-CDMA systems, we can use the spreading code for the desired user to perform channel classification. In [5], it was presented a semi-blind channel identification based on the following semi-blind regularized LS optimization:

$$\hat{\tilde{\mathbf{p}}}_m=\arg\min_{\mathbf{p}}\frac{1}{AGN_t}\underbrace{\left\|\mathbf{r}_{N_t}-\mathbf{X}_{N_t}^m\mathbf{p}\right\|^2}_{Training-based}+\alpha\cdot\underbrace{\left(\mathbf{p}^H\mathbf{\Pi}_m\mathbf{p}\right)}_{Blind-based} \quad (8)$$

Where α is some positive constant [5]

$$\hat{\tilde{\mathbf{p}}}_m=\left[\mathbf{p}_m(0)^T,\cdots,\mathbf{p}_m(q_m)^T\right]^T$$

$$\mathbf{r}_{N_t}=\left[\mathbf{r}(0)^T,\cdots,\mathbf{r}((N_t-1)G)^T\right]^T$$

$$\mathbf{X}_{N_t}^m=\left[\tilde{\mathbf{X}}_{N_t}^m\otimes I_A\right]_{AGN_t\,x\,A(q_m+1)};\ \mathbf{I}_{A\,(A\,x\,A)}\ \text{is the identity matrix}$$

$$\tilde{\mathbf{X}}_{N_t}^m=\begin{bmatrix}x_m(0) & 0 & \cdots & 0\\ \vdots & x_m(0) & \cdots & \vdots\\ \vdots & \vdots & \ddots & \vdots\\ x_m((N_t-1)G) & \vdots & \cdots & x_m((N_t-1)G-q_m)\end{bmatrix}$$

$$x_m(n)=\sum_{k=0}^{N_b-1}b_m(k)\cdot c_m(n-kG)$$

$$\mathbf{\Pi}_m = \mathbf{C}_m^H \cdot \tilde{\tilde{\mathbf{\Xi}}}^H \cdot \tilde{\tilde{\mathbf{\Xi}}} \cdot \mathbf{C}_m \; ; \mathbf{C}_m = \left[\tilde{\tilde{\mathbf{C}}}_m \otimes \mathbf{I}_A\right]_{ALG\,x\,A\left(q_m+1\right)}$$

$$\tilde{\tilde{\mathbf{C}}}_m = \begin{bmatrix} c_m(0) & & & 0 \\ \vdots & c_m(0) & & \\ c_m(G-1) & \vdots & \ddots & \\ & c_m(G-1) & & c_m(0) \\ & & \ddots & \vdots \\ & & & c_m(G-1) \\ 0 & \cdots & \cdots & 0 \end{bmatrix}_{LG\,x\left(q_m+1\right)}$$

$$\tilde{\tilde{\mathbf{\Xi}}} = \begin{bmatrix} \hat{\tilde{\Xi}}_\mu & & \\ \vdots & \ddots & \hat{\tilde{\Xi}}_\mu \\ \hat{\tilde{\Xi}}_1 & \vdots & \\ & \ddots & \hat{\tilde{\Xi}}_1 \end{bmatrix}_{(AG\mu-\xi)(\mu+L-1)\,x\,AGL} \quad ; \hat{\mathbf{U}}_n^H = \left[\hat{\tilde{\Xi}}_1, \cdots, \hat{\tilde{\Xi}}_\mu\right]_{(AG\mu-\xi)\,x\,AG\mu}$$

Whose solution is given by [11]:

$$\hat{\tilde{\tilde{\mathbf{p}}}}_m = \left(\frac{1}{AGN_t}\mathbf{X}_{N_t}^{m\,H}\mathbf{X}_{N_t}^{m} + \alpha\,\mathbf{\Pi}_m\right)^{-1} \cdot \left(\frac{1}{AGN_t}\mathbf{X}_{N_t}^{m\,H}\mathbf{r}_{N_t}\right) \quad (9)$$

V. Semi-blind Constant Modulus Algorithm with Channel Estimation

As presented in [5], SBCMACI first computes the subspace space-time beamforming weight vector for the *m*th user by:

$$\hat{\mathbf{w}}_{m,sub} = \hat{\mathbf{U}}_s \cdot \hat{\mathbf{\Lambda}}_s^{-1} \cdot \hat{\mathbf{U}}_s^H \cdot \mathbf{C}_m \cdot \hat{\tilde{\tilde{\mathbf{p}}}}_m = \mathbf{\Gamma} \cdot \mathbf{C}_m \cdot \hat{\tilde{\tilde{\mathbf{p}}}}_m \quad (10)$$

and then performs the following semi-blind regularized LS iterative procedure:

i. Initialize $\mathbf{w}_m^0 = \hat{\mathbf{w}}_{m,sub}$ (11)

ii. Generate $\tilde{b}_m^{(i)}$, a sequence that contains the N_t training symbols and the $N_b - N_t$ estimated data symbols:

$$\tilde{b}_m^{(i)} = \left\{ b_m(0), \cdots, b_m(N_t-1), \frac{\mathbf{w}_m^{(i)H} \cdot \mathbf{r}_\mu(N_t)}{\left|\mathbf{w}_m^{(i)H} \cdot \mathbf{r}_\mu(N_t)\right|}, \cdots, \frac{\mathbf{w}_m^{(i)H} \cdot \mathbf{r}_\mu(N_b-1)}{\left|\mathbf{w}_m^{(i)H} \cdot \mathbf{r}_\mu(N_b-1)\right|} \right\} \quad (12)$$

iii. Compute

$$\mathbf{w}_m^{(i+1)} = \mathbf{\Gamma} \cdot \underbrace{\left(\frac{1}{N_b}\sum_{k=0}^{N_b-1} \tilde{b}_m^{(i)*}(k) \cdot \mathbf{r}_\mu(k)\right)}_{\tilde{\mathbf{P}}_{N_b}^{m\,(i)}} = \mathbf{\Gamma} \cdot \tilde{\mathbf{P}}_{N_b}^{m\,(i)} \quad (13)$$

iv. Determine $\varepsilon(i) = \left\|\mathbf{w}_m^{(i+1)} - \mathbf{w}_m^{(i)}\right\|^2 \Big/ \left\|\mathbf{w}_m^{(i)}\right\|^2$ (14)

v. Repeat ii. to iv until $\varepsilon(i) < \varepsilon_w$

Where ε_w is some small positive constant.

VI. Recursive Least Squares Algorithm

RLS can also be used to obtain the spatial-temporal beamforming weight vector, $\hat{\mathbf{w}}_m$. In the following, we describe briefly the algorithm, for additional information see [13].

i. Initialize $\mathbf{w}_m^0 = \mathbf{0}$ and $\hat{\mathbf{R}}_{N_t}^{-1} = \left(\sigma^2\right)^{-1} \cdot \mathbf{I}_{u \cdot A \cdot G_p}$ (15)

ii. Compute $\mathbf{K}_{gain}(k) = \dfrac{\lambda^{-1} \cdot \hat{\mathbf{R}}_{N_t}^{-1} \cdot \mathbf{r}_\mu(k)^*}{1 + \lambda^{-1} \cdot r_\mu(k)^T \cdot \hat{\mathbf{R}}_{N_t}^{-1} \cdot \mathbf{r}_\mu(k)^*}$ (16)

iii. Determine $\varepsilon(k) = b_m(k) - \mathbf{r}_\mu(k)^T \cdot \hat{\mathbf{w}}_m^{k-1}$ (17)

iv. Compute $\mathbf{w}_m^k = \mathbf{w}_m^{k-1} + \mathbf{K}_{gain}(k) \cdot \varepsilon(k)$ (18)

v. Update $\hat{\mathbf{R}}_{N_t}^{-1} = \lambda^{-1} \cdot \left\{\hat{\mathbf{R}}_{N_t}^{-1} - \mathbf{K}_{gain}(k) \cdot \mathbf{r}_\mu(k)^T \cdot \hat{\mathbf{R}}_{N_t}^{-1}\right\}$ (19)

Where λ is the forgetting factor.

VII. Simulation Results

In this section, we investigate the performance of the presented semi-blind beamspace-time receiver in a microcell scenario using the GBSBEM model for different training sequence lengths, different number of antennas and in a near-far scenario ($NF = \gamma_{u \neq m}/\gamma_m$), and we compare the results with the training-based beamspace-time RLS receiver.

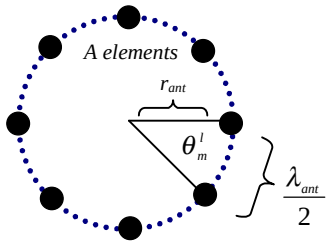

$$a\left(\theta_m^l\right) = \left[\, e^{-j\cdot\frac{2\pi}{\lambda_{ant}}\cdot r_{ant}\cdot\cos\left(\theta_m^l - 2\pi\right)}, \cdots, e^{-j\cdot\frac{2\pi}{\lambda_{ant}}\cdot r_{ant}\cdot\cos\left(\theta_m^l - \frac{2\pi}{A}\right)} \,\right]$$

Figure 3 Circular Antenna Array

For the simulations, we consider an asynchronous DS-CDMA system with complex spreading operating at 2GHz. There are 8 QPSK modulated users (*M*=8) per cell, each one transmitting frames with 200 symbols (N_b=200). The chip rate is 3.84 Mcps, the symbol rate is 256 Kbps and the processing gain is 15 (*G*=15). The spreading sequences are Gold-like and are normalized to unit energy. It is considered that the frame duration is short compared with the coherence time of the channel. The cell ratio is 500 *m*, and the users are randomly positioned around the cell between 50 *m* and 500 *m* ($50 \le d_m \le 500$) and with angles between –180° and 180°. We assume for all the users that the propagation delay is 3.33 μs (~13 chip) and L_m=4. The AOA of the strongest path of the

desired signal is kept 150^o ($\theta_m^{1_m} = 150^\circ$) for all the simulations. The base station employs a circular array antenna (see Fig.3) with equally spaced elements ($\lambda_{ant}/2$) and the SNR at bit level for each antenna element is 6dB (Fig.4-6 and Fig.8-9). The signal space is estimated by using MDL method [12]. The results are obtained computing 500 frames per evaluated parameter (*SNR*, N_t etc). For all simulations, we consider μ=1, L=2, α=0.01 and $\varepsilon_w = 10^{-5}$.

In Fig.4 and Fig.5, the bit error rate (BER) and the mean square error (MSE) of the proposed receiver for different number of antenna elements are presented. The results show that it is possible to reduce MAI and ICI and explore multipath diversity with few training symbols. It also shows the performance degradation in overload scenarios (A<M) [1].

In Fig.6, we compare the performance of the beamspace-time SBCMACI against the beamspace-time RLS varying the length of the training sequence. The result shows that the proposed receiver outperforms the beamspace-time RLS and that it can improve the near-far resistance increasing the number of training symbols.

Comparison between SBCMACI and RLS beamspace-time receivers varying the SNR in different near-far scenarios (NF=0/5dB) using different training lengths (N_t=4-6) is presented in Fig.7. Again, the performance of the proposed receiver outperforms the beamspace-time RLS receiver.

Finally, in Fig.8 and Fig.9, we show the radiation patterns and constellation diagrams of the last evaluated frame for a 9 element circular antenna array (A=9) with NF=0dB, SNR=6dB and two different training lengths (N_t=2/6).

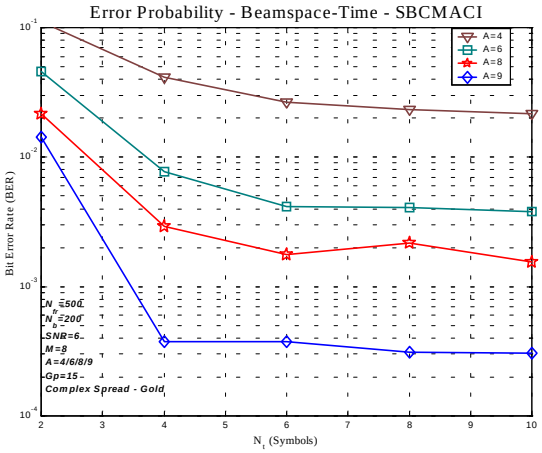

Figure 4 BER of Beamspace-time SBCMACI varying number of training symbols and antennas elements for SNR= 6dB (M=8 and NF=0dB)

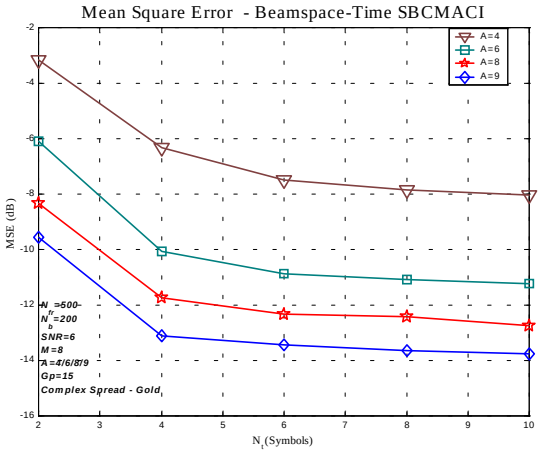

Figure 5 MSE of Beamspace-time SBCMACI varying number of training symbols and antennas elements for SNR= 6dB (M=8 and NF=0dB)

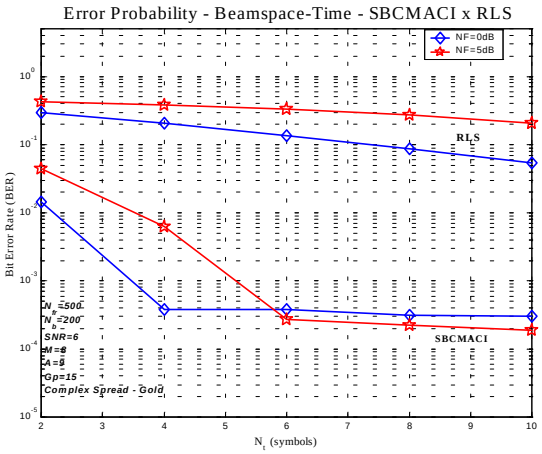

Figure 6 BER of Beamspace-time SBCMACI and RLS varying number of training symbols and Near-Far factor for SNR=6dB (M=8 and A=9)

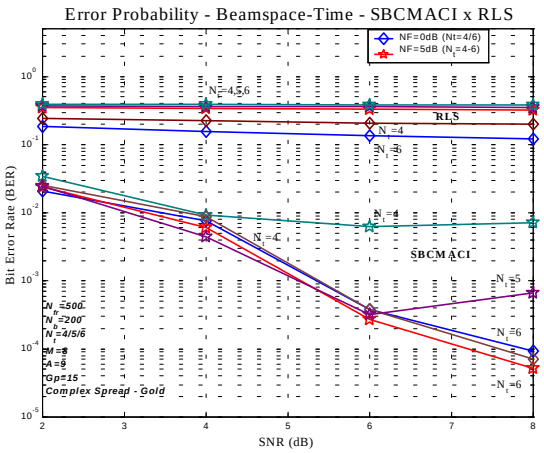

Figure 7 BER of Beamspace-time SBCMACI and RLS varying SNR (M=8, A= 9, N_t=4-6 & NF=0dB/5dB)

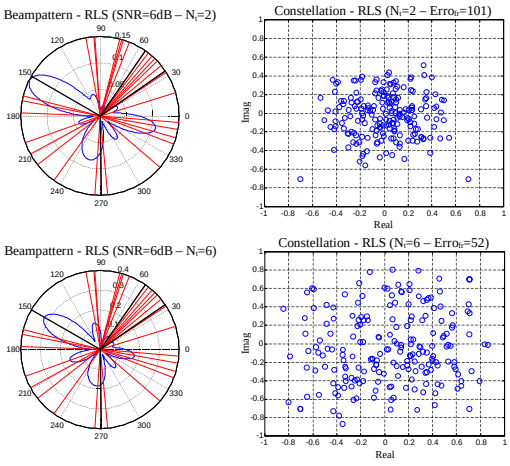

Figure 8 Radiation Pattern and Constellation Diagram for RLS with SNR=6dB (M=8, N_t= 2/6, A=9 & NF=0dB)

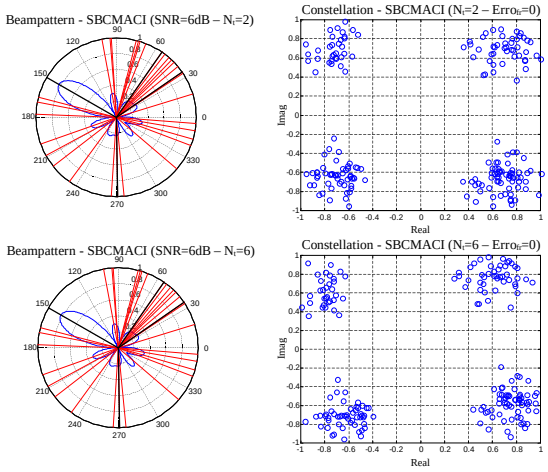

Figure 9 Radiation Pattern and Constellation Diagram for SBCMACI with SNR=6dB (M=8, N_t= 2/6, A=9 & NF=0dB)

VIII. Conclusion

The 3rd generation of cellular systems will support a wide range of services in different environments, being necessary different type of cells to attend such requirement. The microcell-macrocell hierarchical cellular architecture is a promising technique to provide an efficient way to integrate different cell sites and attend the requirements of next cellular generation. In this architecture, microcells will be responsible to provide high spectrum efficiency and high traffic capacity to low mobility users. However, due to the frequency reuse factor equal to one, the use of the hierarchical architecture brings some problems as cross-layer interference.

The use of spatial-temporal antenna array receivers in the microcells can mitigate this problem, offering efficient handover, capacity enhancement, and reduction of near-far effect between layers of the hierarchical cellular architectures.

In this paper, we have investigated the performance of a semi-blind SBCMACI spatial-temporal beamforming receiver in a microcell with low mobility and high data rate users. We have performed simulations considering an asynchronous high data rate WCDMA system employing complex spreading and a circular antenna array in a near-far scenario. The results show a significant performance improvement and a reduction of required training symbols (even in a near-far scenario) when compared against a receiver employing training-based spatial-temporal RLS beamforming.

References

[1] A. Paulraj and C. B. Papadias, “Space-Time Processing for Wireless Communications”, IEEE Signal Processing Magazine, vol.14, no.6, pp.49-83, Nov. 1997.

[2] H. Krim and M. Viberg, “Two Decades of Array Signal Processing Research, The Parametric Approach,” IEEE Signal Processing Magazine, vol.13, no.3, pp.67-94, Jul. 1996.

[3] L. C. Godara, “Application of Antenna Arrays to Mobile Communications, Part II: Beam-Forming and Direction of Arrival Considerations”, Proceedings of IEEE, vol.85, no. 8, pp.1031-1060, Aug. 1997.

[4] I. R. S. Casella, E. S. Sousa and P. J. E. Jeszensky, “Semi-Blind Beamspace-Time Interference Cancellation using Subspace Channel Identification for DS-WCDMA Systems”, submitted to Personal Indoor Mobile Radio Communication, 2002

[5] R. A. Pacheco and D. Hatzinakos, “Semi-Blind Spatial Temporal Equalization and Multi-user Detection for DS-CDMA Systems”, IEEE Signal Processing Advances in Wireless Communications, pp.126-129, 2001.

[6] 3GPP, “Universal Mobile Telecommunications Systems - Spreading and Modulation (FDD)”, ETSI TS 125 213 v3.3.0, Jun. 2000.

[7] J. C. Camacho and D. L. Rodriguez, “Performance of a New Microcell/Macrocell Cellular Architecture with CDMA Access”, Vehicular Technology Conference, pp.483-486, 2000.

[8] G. V. Tsoulos, M. A. Beach and S. C. Swales, “Application of Adaptive Antenna Technology to Third Generation Mixed Cell Radio Architectures”, Vehicular Technology Conference, pp.615-619, 1994.

[9] E. H. Dinan and B. Jabbai, “Spreading Codes for Direct Sequence CDMA and Wideband CDMA Cellular Networks”, IEEE Communications Magazine, vol.3, no.9, pp.48-54, Sep. 1998.

[10] J. C. Liberti and T. S. Rappaport, “A Geometrically Based Model for Line of Sight Multipath Radio Channels”, IEEE Vehicular Technology Conference, pp.844-848, 1996.

[11] E. Moulines, P. Duhamel, J.-F. Cardoso, and S. Mayrargue, “Subspace Methods for the Blind Identification of Multichannel FIR Filters”, IEEE Trans. Signal Processing, vol.43, no.2, pp.516-525, Feb. 1995.

[12] M. Wax and I. Ziskind, “Detection of the Number of Coherent Signals by the MDL Principle”, IEEE Trans. on Acoustics, Speech and Signal Processing, vol.37, no.8, pp.1190-1196, Aug. 1989.

[13] S. Haykin, “Adaptive Filter Theory”, Prentice-Hall, Englewood Cliffs, NJ, 3rd edition, 1996.